

# Optical Engineering

OpticalEngineering.SPIEDigitalLibrary.org

## **Whispering-gallery modes observed in elastic scattering from submerged high-refractive-index silica microspheres**

Hasan Yılmaz  
Huzeyfe Yılmaz  
Mehmet Selman Tamer  
Oğuzhan Gürlü  
Mohammed Sharif Murib  
Ali Serpengüzel

**SPIE.**

Hasan Yılmaz, Huzeyfe Yılmaz, Mehmet Selman Tamer, Oğuzhan Gürlü, Mohammed Sharif Murib, Ali Serpengüzel, "Whispering-gallery modes observed in elastic scattering from submerged high-refractive-index silica microspheres," *Opt. Eng.* **56**(12), 126110 (2017), doi: 10.1117/1.OE.56.12.126110.

# Whispering-gallery modes observed in elastic scattering from submerged high-refractive-index silica microspheres

Hasan Yılmaz,<sup>a,†</sup> Huzeyfe Yılmaz,<sup>a,‡</sup> Mehmet Selman Tamer,<sup>b,§</sup> Oğuzhan Gürlü,<sup>b</sup> Mohammed Sharif Murib,<sup>a,¶</sup> and Ali Serpengüzel<sup>a,\*</sup>

<sup>a</sup>Koç University, Department of Physics, Microphotonics Research Laboratory, Rumelifeneri Yolu, Sariyer, Istanbul, Turkey

<sup>b</sup>Istanbul Technical University, Department of Physics, Faculty of Sciences and Letters, Maslak, Istanbul, Turkey

**Abstract.** The effect of the discrete values of the refractive index of the surrounding medium on the spectral behavior of the whispering-gallery modes (WGMs) in the elastic scattering spectra of high-refractive-index silica microspheres submerged in fluids, such as air, water, and glycerol, is studied. The elastic scattering spectral measurements, as well as the spectral autocorrelation analysis of these elastic scattering spectra show that the spectral-mode spacing, the spectral-mode density, and the spectral-mode definition of the WGMs decrease as the refractive index of the surrounding fluid increases. We believe that this work opens up the way for optofluidic applications of high-refractive-index silica microsphere-based guided wave optics. © 2017 Society of Photo-Optical Instrumentation Engineers (SPIE) [DOI: 10.1117/1.OE.56.12.126110]

Keywords: fiber optics; fiber optic sensors; Mie theory; resonators; scattering; spectroscopy.

Paper 170803 received May 26, 2017; accepted for publication Oct. 10, 2017; published online Dec. 27, 2017.

## 1 Introduction

Half a century elapsed since the proposal of the cavity alteration of the spontaneous emission for radio waves by Purcell.<sup>1</sup> Since then, optical microresonators have found many applications in photonics.<sup>2</sup> Microspheres<sup>3,4</sup> with whispering-gallery modes (WGMs)<sup>5</sup> with large quality-factors ( $Q$ -factors)<sup>6</sup> coupled to optical waveguides<sup>7</sup> have found applications in optical fiber communication and sensing<sup>8</sup> as microlasers,<sup>9</sup> channel-dropping filters,<sup>10</sup> optical switches,<sup>11,12</sup> tunable filters,<sup>13</sup> Raman lasers,<sup>14</sup> rotation sensors,<sup>15</sup> and biosensors.<sup>16</sup>

In addition to dielectric spheres, semiconductor, e.g., silicon, microspheres have been used in channel dropping<sup>17</sup> and considered for optoelectronic applications.<sup>18,19</sup> Silicon microspheres have been used for optical modulation applications in air<sup>20</sup> and in nematic liquid crystals.<sup>21</sup> Germanium microspheres<sup>22</sup> were studied for electronic- and photonic-integration applications. Semiconductor microspheres are extremely important due to their high refractive indices, which enables the realization of small devices with a high performance. However, most semiconductor materials are not appropriate for visible-light applications due to their absorption losses.

Ultrafine sensing<sup>23</sup> and biomolecular agent detection<sup>24</sup> are also interesting for optical miniature biosensors,<sup>25</sup> which utilize high  $Q$ -factor microsphere resonators.<sup>26</sup> These sensors

have taken advantage of either the wavelength shift or the linewidth broadening of WGMs, induced by the adsorption of biomolecules onto the surface of the microsphere.<sup>27</sup> While the wavelength shift of a WGM is caused either by a change in the refractive index or the size of the microsphere,<sup>28</sup> the linewidth broadening is frequently due to the scattering losses that affect the cavity  $Q$ -factor.<sup>29</sup> Because of the importance of improving detector performance, increasing the sensitivity of these devices is crucial. Enhanced sensitivity of microsphere sensors can result from coating the microsphere with a high-refractive-index surface layer in order to increase the frequency-shift sensitivity.<sup>30</sup> Ultrasensitive chemical sensors have also been fabricated using film-coated microspheres.<sup>31</sup> Microspheres have also been used to measure changes in the surrounding liquid medium's refractive index<sup>32</sup> by dynamically tracking the redshift of the WGMs.

In this paper, we report, for the first time to the best of our knowledge, the static measurement of surrounding fluid's refractive index on the WGM spectral behavior, such as mode spacing ( $\Delta\lambda$ ), mode density, and mode definition [signal-to-background (BG) ratio] of high-refractive-index ( $N_1 = 1.9$ )-doped silica microspheres, submerged in various fluids, placed on a pure silica optical fiber half coupler (OFHC), and excited with a tunable dye laser in the visible spectral region.

We believe that this work opens a way for optofluidic applications, such as optofluidic dye lasers,<sup>33</sup> optofluidic switches,<sup>34</sup> tunable filters,<sup>35</sup> electrowetting based lenses,<sup>36</sup> and various biochemical sensors.<sup>37</sup>

## 2 Whispering-Gallery Modes of Spherical Optical Resonators

WGMs in a spherical cavity are explained by Lorenz<sup>38</sup>–Mie<sup>39</sup> theory. When the optical path inside a cavity is equal to an integer multiple of wavelength, a standing wave occurs in the cavity. For large microspheres ( $a \gg \lambda$ ), with refractive

\*Address all correspondence to: Ali Serpengüzel, E-mail: [aserpenguzel@ku.edu.tr](mailto:aserpenguzel@ku.edu.tr)

<sup>†</sup>Present address: Yale University, Department of Applied Physics, New Haven, Connecticut, United States

<sup>‡</sup>Present address: University of Washington, Department of Electrical and Systems Engineering, St. Louis, Missouri, United States

<sup>§</sup>Present address: Delft University of Technology, Department of Precision and Microsystems Engineering, Delft, The Netherlands

<sup>¶</sup>Present address: Gent University/IMEC, INTEC Technologiepark, Department of Information Technology, Ghent, Belgium

index  $N_1$  and radius  $a$ , the condition for the WGM is  $k_1 a = 2\pi a N_1 / \lambda = n$ , where  $k_1$  is the propagation vector in the microsphere,  $\lambda / N_1$  is the wavelength of light in the microsphere, and  $n$  is an integer quantum (polar mode) number.<sup>40</sup> A better approximation of the resonance condition is given by  $k_1 a = k N_1 a = n + 1.856n^{1/3} - M / (M^2 - 1)^{1/2}$ .<sup>32</sup>

Frequently, a dimensionless size parameter  $x = 2\pi N a / \lambda$  is defined to be used in expressions of this system. The standing wave condition can then be expressed as a function of the size parameter, the integer quantum (polar mode) number  $n$ , and the relative refractive index  $M = N_1 / N$ , where  $N$  is the refractive index of the surrounding medium. As shown in the sketch of Fig. 1(a), the WGMs defined by radial ( $l$ ), polar ( $n$ ), and azimuthal ( $m$ ) mode numbers exhibit a spectral-mode spacing  $\Delta\lambda = \lambda^2 \arctan[(M^2 - 1)^{1/2}] / 2\pi a N (M^2 - 1)^{1/2}$ , i.e., a spectral distance between two WGMs with the same

radial mode number ( $l$ ) and consecutive polar mode number ( $n$ ).<sup>41</sup> The mode density of the WGMs is another important spectral parameter and decreases with decreasing refractive index contrast between the inside and the outside of the sphere. As shown in the sketch of Fig. 1(b), the spectral-mode definition (ratio of WGM signal-to-BG signal) of the WGMs can be measured by performing an autocorrelation<sup>42</sup> analysis of the elastic scattering signal.

The spectral autocorrelation analysis related to elastic scattering spectra was previously performed to study particles in suspension,<sup>43</sup> rough surfaces,<sup>44,45</sup> polymer films,<sup>46</sup> semicontinuous metal films,<sup>47</sup> and random lasers.<sup>48</sup> Here, we are using spectral autocorrelation analysis for extracting the spectral-mode spacing, spectral-mode density, and spectral-mode definition. The spectral autocorrelation analysis is performed using the autocorrelation function on the measured elastic scattering spectra.<sup>49</sup>

The slope of the autocorrelation signal increases with an increase of the BG signal with respect to the WGM signal. The closer the autocorrelation baseline to the horizontal, the higher is the spectral-mode definition of the WGMs.<sup>50</sup> As shown in Fig. 1(c), the minimum of the second derivative of the autocorrelation spectra can be used to find the maximum of the autocorrelation spectra.<sup>51</sup>

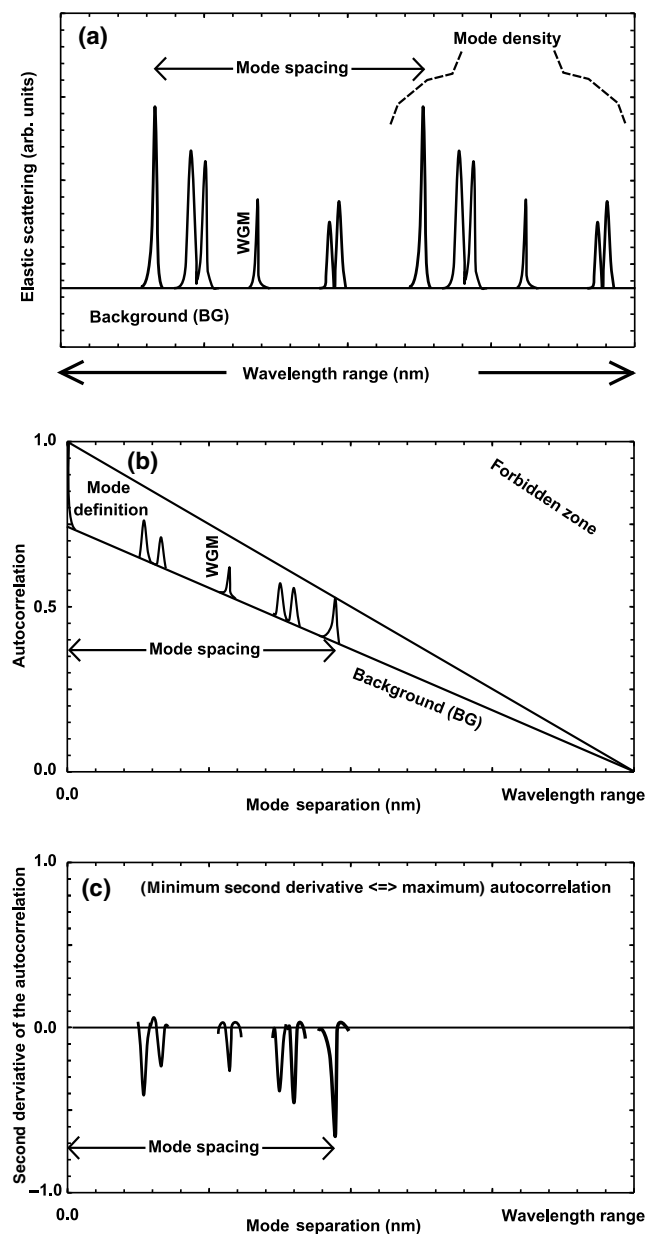


Fig. 1 Sketch of (a) elastic scattering, (b) its autocorrelation, and (c) second derivative of the autocorrelation spectra.

### 3 Experimental Setup of Elastic Scattering from Silica Microspheres

A schematic of our experimental setup is shown in Fig. 2. A visible tunable dye laser operating with DCM laser dye with a lasing spectrum between 615 and 655 nm is pumped by a frequency-doubled (532 nm) Nd:YAG laser. The dye laser output is coupled to a silica single-mode optical fiber (SMOF) with a refractive index of  $N_{\text{SMOF}} = 1.46$ , which is coupled to an SMOF OFHC in order to couple light to the high-refractive-index ( $N_1 = 1.9$ ) silica microsphere with a radius of  $12.75 \mu\text{m}$ .

The 90-deg elastic light scattering from the silica microsphere is detected by imaging the silica microsphere on to a photomultiplier tube with an optical microscope. The wavelength of the laser light is tuned between 632 and 640 nm with 4-pm steps. The intensity of scattered light is recorded per each scan step leading to 2000 data points per spectrum. A beam splitter is used to observe and position the microsphere to an optimal position for sufficient light coupling. With a randomly polarized input light, both transverse electric (TE) and transverse magnetic (TM) modes are excited, and rich elastic scattering spectra are observed. The measured elastic scattering spectra contain a collection of TE

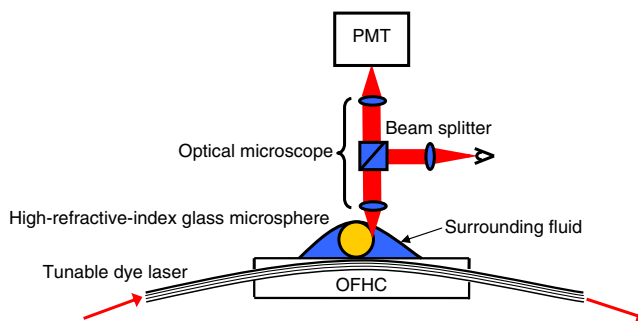


Fig. 2 The schematic of the experimental setup showing the silica microsphere placed on the OFHC.

and TM WGMs with different radial mode numbers. The number of observed WGMs, as well as their  $Q$ -factors, depends on the resolution of the measurement setup.

#### 4 Elastic Light Scattering Spectra from Silica Microspheres Immersed in Fluids

The silica microsphere is investigated first in air. Figure 3(a) shows the 90-deg elastically scattered spectrum for a silica microsphere in air. WGMs are observed as peaks in the 90-deg elastic scattering spectrum. Due to the high refractive index ( $N_1 = 1.9$ ) of the silica microspheres, WGMs have narrow spectral linewidths and are spectrally dense with a spectral-mode spacing of  $\Delta\lambda = 3.24$  nm.

Observation of WGMs in water is important for biochemical sensing applications, since sensing experiments are mostly performed in aqueous solutions. Figure 3(b) shows the 90-deg elastically scattered spectrum for a silica microsphere in water ( $N = 1.33$ ). When compared to air, the spectral-mode spacing ( $\Delta\lambda$ ) has decreased due to the effective

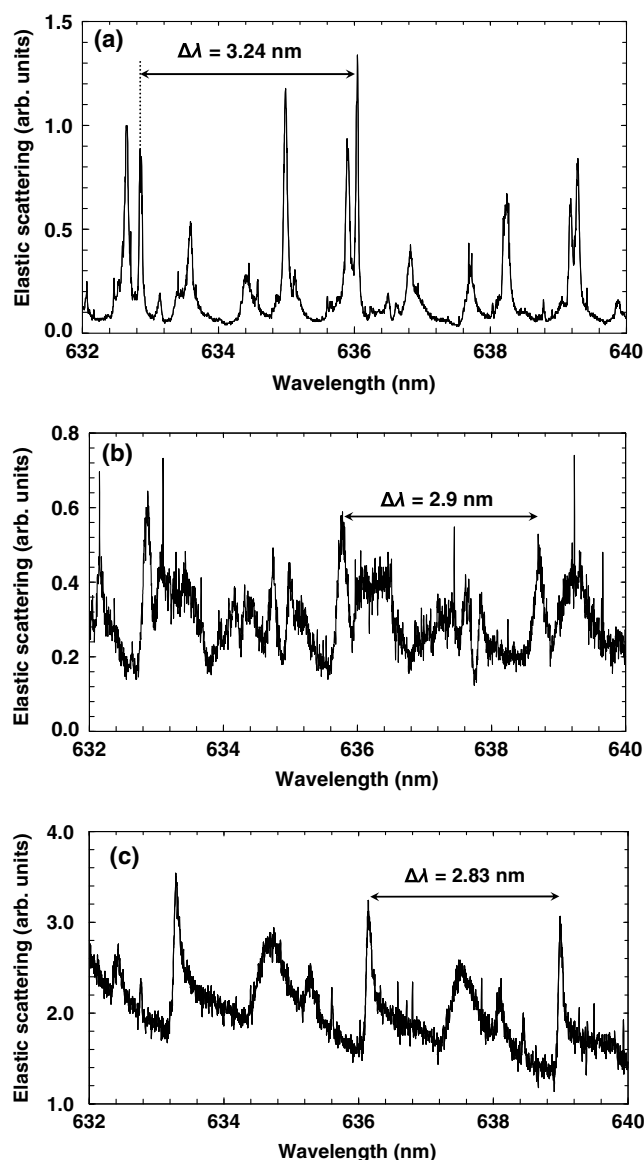


**Fig. 3** The 90-deg elastic scattering spectra of silica microsphere in (a) air, (b) water, and (c) glycerol.

refractive index decrease of the silica microsphere in water. WGMs extend into the surrounding medium due to higher refractive index of water compared to air, which is observed as a redshift and reduced mode spacing in the spectrum.<sup>52</sup> When compared to air, the BG of the elastic scattering signal in water has increased due to increased scattering from the surface of the OFHC.

Glycerol is a high-refractive-index ( $N = 1.43$ ) transparent medium in the visible spectrum. Figure 3(c) shows the 90-deg elastic scattered light spectrum for a silica microsphere in glycerol. Glycerol has a higher refractive index compared to air and water. The high refractive index of glycerol enhances the scattering from the surface of the OFHC, thereby the BG signal increases. The WGM spectral-mode spacing is smaller compared to both water and air immersion due to the effective refractive index decrease of the silica

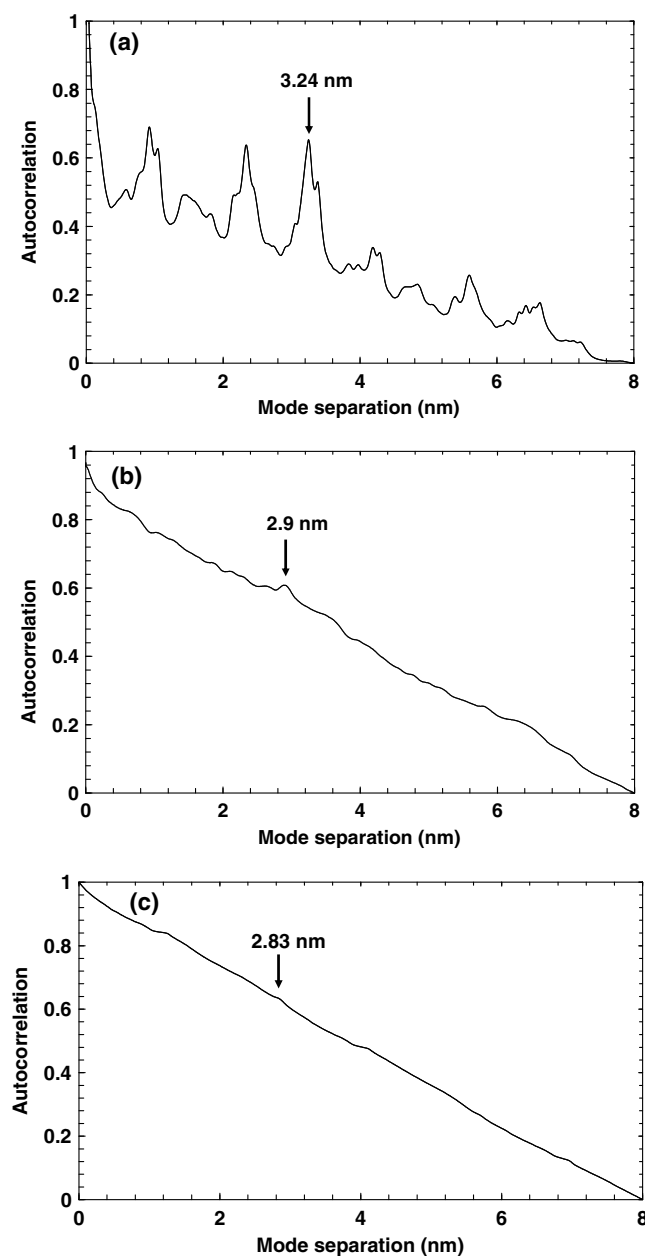


**Fig. 4** Elastic scattering autocorrelation spectra of silica microsphere in (a) air, (b) water, and (c) glycerol.

microsphere in glycerol. When compared to water, the decreased WGM spectral definition (ratio of WGM signal-to-BG signal) in glycerol is due to the increase of the BG scattering from the surface of the OFHC.

The spectral density of WGMs also decreases with increasing refractive index of the surrounding fluid medium. For the microsphere in air [Fig. 3(a)], there are  $\sim 13$  perceptible WGMs, whereas in water [Fig. 3(b)], the number of perceptible WGMs is 7, and in glycerol [Fig. 3(c)], the number of perceptible WGMs per mode spacing is 4, respectively. Air ( $N = 1.00$ ) with the highest refractive index contrast with the silica fiber ( $N_{\text{SMOF}} = 1.46$ ) gives rise to the best optical confinement, resulting in the maximum number of perceptible WGMs.

## 5 Autocorrelation Spectra of the Elastic Scattering from Silica Microspheres

To study the correlation of the elastic scattering spectra with the silica microsphere size, an autocorrelation analysis is used in the 90-deg elastic scattering spectra. Figures 4(a)–4(c) show the autocorrelation analysis of the 90-deg elastic scattering spectra of the silica microsphere submerged in air, water, and glycerol, respectively. The WGM spectral-mode spacing ( $\Delta\lambda$ ) is clearly visible for the silica microsphere in air, water, and glycerol, i.e.,  $\Delta\lambda = 3.24$  nm,  $\Delta\lambda = 2.9$  nm, and  $\Delta\lambda = 2.83$  nm, respectively. As the refractive index of the outside fluid increases, the WGM spectral-mode spacing ( $\Delta\lambda$ ) decreases.

WGM spectral definition can be measured by comparing the WGM signal quality with the BG signal. The slope of the autocorrelation baseline is minimum [0.4/8 nm in Fig. 4(a)] in air and [0.9/8 nm in Fig. 4(b)] in water, and maximum [1.0/8 nm in Fig. 4(c)] in glycerol, so that the WGMs in air have the best spectral-mode definition.

The WGM spectral density decreases with the increase of the surrounding fluid medium's refractive index ( $N$ ), as evidenced in the autocorrelation spectrum for the microsphere in air [Fig. 4(a)] with  $\sim 13$  WGMs, in water [Fig. 4(b)] with  $\sim 4$  WGMs, and in glycerol [Fig. 4(c)] with  $\sim 2$  WGMs perceptible in one-mode spacing, respectively. Again air ( $N = 1.00$ ) with the highest refractive index contrast, when compared to the silica optical fiber ( $N_{\text{SMOF}} = 1.46$ ), shows the highest WGM-mode density.

The second derivative of the autocorrelation spectra is given in Figs. 5(a)–5(c) for air, water, and glycerol, respectively. Using the minimum of the second derivative, it is possible to locate the peaks in autocorrelation spectra of Fig. 4. The second-derivative spectra in Figs. 5(a) and 5(b) locate the mode spacing in autocorrelation peaks of Figs. 4(a) and 4(b). The second-derivative spectrum in Fig. 5(c), however, locates as the minimum another autocorrelation peak for our case of unpolarized spectroscopy. TE- or TM-polarized spectroscopy might be better suited for recovering the spectral-mode spacing of  $\Delta\lambda = 2.83$  nm for the glycerol as well.

In addition, in Figs. 5(a) and 5(b) the minimum of the second derivative gives us the correct mode spacing values, whereas, in Fig. 5(c), the minimum of the second derivative gives us some other spectral value. This false positive can be avoided, if the radius of the microsphere is reduced so that only one radial order is preserved, resulting in a mode

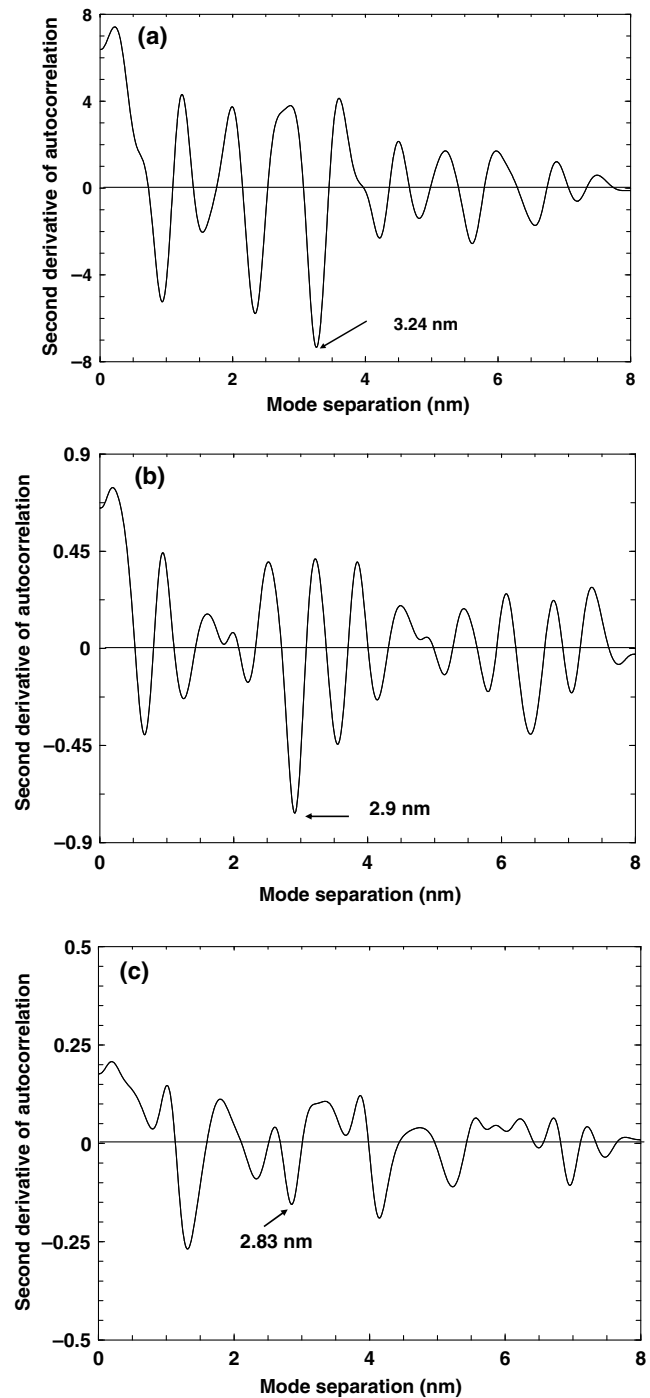


**Fig. 5** Second derivative of autocorrelation spectra of silica microsphere in (a) air, (b) water, and (c) glycerol.

spacing free of other radial order modes, analog to the free-spectral range of a Fabry–Pérot resonator.

Compared to the dynamic WGM redshift method,<sup>32</sup> which continuously acquires spectral data, our method is static and takes snapshots of the elastic scattering spectra and can be implemented for cases, when continuous data acquisition is not needed.

## 6 Conclusions

Observation of the WGMs of free-standing monolithic high-refractive-index silica microspheres immersed in different

amorphous fluids has been demonstrated. The spectrally measured WGM-mode spacing ( $\Delta\lambda$ ) compares favorably with the optical size of the high-refractive-index silica microsphere and is also evidenced by the spectral autocorrelation analysis of the elastic scattering spectra. The decrease in the spectral-mode density of WGMs with increasing refractive index of the surrounding fluid environment is due to the decrease of the optical confinement, resulting in a decrease in the number of WGMs. The increase of the BG with respect to WGM signal is proportional to the refractive index of the outside medium, which increases the scattering from the surface of the OFHC, resulting in a decrease of the WGM spectral definition. This work presents an analysis method of the WGM spectra of high-refractive-index silica microsphere—silica optical fiber system immersed in static fluid surroundings and opens up the way for a variety of optofluidic applications of high-refractive-index silica microsphere-based guided wave optics.

### Acknowledgments

We would like to acknowledge the partial support of this research by the Scientific and Technological Research Council of Turkey (TUBITAK) Grant No. EEEAG-106E215 and the European Commission Grants Nos. FP6-IST-003887 NEMO and FP6-IST-511616 PHOREMOST.

### References

1. E. M. Purcell, "Spontaneous emission probabilities at radio frequencies," *Phys. Rev.* **69**, 37 (1946).
2. R. K. Chang and A. J. Campillo, *Optical Processes in Microcavities*, World Scientific, Singapore (1996).
3. R. E. Benner et al., "Observation of structure resonances in the fluorescence spectra from microspheres," *Phys. Rev. Lett.* **44**, 475–478 (1980).
4. A. Serpengüzel and A. W. Poon, *Optical Processes in Microparticles and Nanostructures: A Festschrift Dedicated to Richard Kounai Chang on His Retirement from Yale University*, World Scientific, Singapore (2011).
5. J. D. Eversole et al., "Spherical-cavity-mode assignments of optical resonances in microdroplets using elastic-scattering," *J. Opt. Soc. Am. A* **7**, 2159–2168 (1990).
6. A. A. Savchenkov et al., "Kilohertz optical resonances in dielectric crystal cavities," *Phys. Rev. A* **70**, 051804 (2004).
7. A. Serpengüzel, S. Arnold, and G. Griffel, "Excitation of resonances of microspheres on an optical fiber," *Opt. Lett.* **20**, 654–656 (1995).
8. J. Pfeifle et al., "Optimally coherent Kerr combs generated with crystalline whispering gallery mode resonators for ultrahigh capacity fiber communications," *Phys. Rev. Lett.* **114**, 093902 (2015).
9. S. Borri et al., "Tunable microcavity-stabilized quantum cascade laser for mid-IR high-resolution spectroscopy and sensing," *Sensors* **16**, 238 (2016).
10. S. I. Shopova, G. Farca, and A. T. Rosenberger, "Microsphere whispering-gallery-mode laser using HgTe quantum dots," *Appl. Phys. Lett.* **85**, 6101–6103 (2004).
11. I. Razdolskiy et al., "Hybrid microspheres for nonlinear Kerr switching devices," *Opt. Express* **19**, 9523–9528 (2011).
12. F. H. Suhailin et al., "Kerr nonlinear switching in a hybrid silica-silicon microspherical resonator," *Opt. Express* **23**, 17263–17268 (2015).
13. G. Gilardi et al., "Liquid-crystal tunable filter based on sapphire microspheres," *Opt. Lett.* **34**, 3253–3255 (2009).
14. I. S. Grudinin and L. Maleki, "Efficient Raman laser based on a CaF<sub>2</sub> resonator," *J. Opt. Soc. Am. B* **25**, 594–598 (2008).
15. P. An et al., "High-Q microsphere resonators for angular velocity sensing in gyroscopes," *Appl. Phys. Lett.* **106**, 063504 (2015).
16. M. S. Murib et al., "Elastic scattering from a sapphire microsphere placed on a silica optical fiber coupler: possible applications to biosensing," *Eur. Phys. J. Spec. Top.* **223**, 1995–2002 (2014).
17. Y. O. Yılmaz et al., "Optical channel dropping with a silicon microsphere," *IEEE Photonics Technol. Lett.* **17**, 1662–1664 (2005).
18. A. Serpengüzel, A. Kurt, and U. K. Ayaz, "Silicon microspheres for electronic and photonic integration," *Photonics Nanostruct. Fundam. Appl.* **6**, 179–182 (2008).
19. M. S. Murib et al., "Polarization behavior of elastic scattering from a silicon microsphere coupled to an optical fiber," *Photonics Res.* **2**, 45–50 (2014).
20. E. Yüce, O. Gürlü, and A. Serpengüzel, "Optical modulation with silicon microspheres," *IEEE Photonics Technol. Lett.* **21**, 1481–1483 (2009).
21. H. Yılmaz and A. Serpengüzel, "Electro-optical modulation with silicon microspheres in liquid crystal," *Proc. SPIE* **8069**, 80690L (2011).
22. P. Wang et al., "Germanium microsphere high-Q resonator," *Opt. Lett.* **37**, 728–730 (2012).
23. I. Teraoka, S. Arnold, and F. Vollmer, "Perturbation approach to resonance shifts of whispering-gallery modes in a dielectric microsphere as a probe of a surrounding medium," *J. Opt. Soc. Am. B* **20**, 1937–1946 (2003).
24. A. Demir and A. Serpengüzel, "Silica microspheres for biomolecular detection applications," *IEEE Proc. Nanobiotechnol.* **152**, 105–108 (2005).
25. G. Righini and S. Soria, "Biosensing by WGM microspherical resonators," *Sensors* **16**, 905 (2016).
26. F. Vollmer and S. Arnold, "Whispering-gallery-mode biosensing: label-free detection down to single molecules," *Nat. Methods* **5**, 591–596 (2008).
27. S. Arnold et al., "Shift of whispering-gallery modes in microspheres by protein adsorption," *Opt. Lett.* **28**, 272–274 (2003).
28. M. R. Foreman, J. D. Swaim, and F. Vollmer, "Whispering gallery mode sensors," *Adv. Opt. Photonics* **7**, 168–240 (2015).
29. H. C. Ren et al., "High-Q microsphere biosensor—analysis for adsorption of rodlike bacteria," *Opt. Express* **15**, 17410–17423 (2007).
30. O. Gaathon et al., "Enhancing sensitivity of a whispering gallery mode biosensor by subwavelength confinement," *Appl. Phys. Lett.* **89**, 223901 (2006).
31. N. Lin et al., "Ultrasensitive chemical sensors based on whispering gallery modes in a microsphere coated with zeolite," *Appl. Opt.* **49**, 6463–6471 (2010).
32. T. Ioppolo, N. Das, and M. V. Ötügen, "Whispering gallery modes of microspheres in the presence of a changing surrounding medium: a new ray-tracing analysis and sensor experiment," *J. Appl. Phys.* **107**, 103105 (2010).
33. W. Song and D. Psaltis, "Pneumatically tunable optofluidic dye laser," *Appl. Phys. Lett.* **96**, 081101 (2010).
34. Y. Gu, G. Valentino, and E. Mongeau, "Ferrofluid-based reconfigurable optofluidic switches for integrated sensing and digital data storage," *Appl. Opt.* **53**, 537 (2014).
35. F. Chen and D. Yao, "Optofluidic tunable plasmonic filter based on liquid-crystal microcavity structures," *J. Mod. Opt.* **61**, 1486–1491 (2014).
36. X. Hu et al., "Electrowetting based infrared lens using ionic liquids," *Appl. Phys. Lett.* **99**, 213505 (2011).
37. Y. Chen et al., "Optofluidic microcavities: dye-lasers and biosensors," *Biomicrofluidics* **4**, 043002 (2010).
38. L. Lorenz, *Oeuvres scientifiques de L. Lorenz, revues et annotées par H. Valentiner*, Tome Premier, Libraire Lehmann et Stage, Copenhagen, p. 403 (1898).
39. G. Mie, "Beiträge zur Optik trüber Medien, speziell kolloidaler Metallösungen," *Ann. Phys.* **330**, 377–445 (1908).
40. C. F. Bohren and D. R. Huffman, *Absorption and Scattering of Light by Small Particles*, Chapter 4, p. 82, Wiley, New York (1983).
41. P. Chýlek, "Resonance structure of Mie scattering: distance between resonances," *J. Opt. Soc. A* **7**, 1609–1613 (1990).
42. M. Lahat, R. Niederjohn, and D. Krubsack, "A spectral autocorrelation method for measurement of the fundamental frequency of noise-corrupted speech," *IEEE Trans. Acoust. Speech Signal Process.* **35**, 741–750 (1987).
43. P. R. Smith, O. Kusmartseva, and R. Naimimohases, "Evidence for particle-shape sensitivity in the correlation between polarization states of light scattering," *Opt. Lett.* **26**, 1289–1291 (2001).
44. W. T. Welford, "Laser speckle and surface roughness," *Contemp. Phys.* **21**, 401–412 (1980).
45. D. D. Duncan and S. J. Kirkpatrick, "The copula: a tool for simulating speckle dynamics," *J. Opt. Soc. Am. A* **25**, 231–237 (2008).
46. J. Holoubek et al., "Light scattering speckle patterns and their correlation properties," *J. Mod. Opt.* **34**, 633–642 (1987).
47. K. Seal et al., "Near-field intensity correlations in semicontinuous metal-dielectric films," *Phys. Rev. Lett.* **94**, 226101 (2005).
48. H. Cao et al., "Probing localized states with spectrally resolved speckle techniques," *Phys. Rev. E* **66**, 025601 (2002).
49. G. E. P. Box et al., *Time Series Analysis: Forecasting and Control*, Chapter 2, p. 21, John Wiley, Hoboken, New Jersey (2015).
50. E. Tsotsas and A. S. Mujumdar, *Modern Drying Technology, Experimental Techniques*, Chapter 6, p. 287, Wiley-VCH Verlag, Weinheim (2009).
51. B. J. de Aragão and Y. Messaddeq, "Peak separation by derivative spectroscopy applied to FTIR analysis of hydrolyzed silica," *J. Braz. Chem. Soc.* **19**, 1582–1594 (2008).
52. L. Shi et al., "Angle-dependent quality factor of Mie resonances in silicon-colloid-based microcavities," *ACS Photonics* **1**, 408–412 (2014).

Hasan Yılmaz received his BSc degree in physics engineering from Istanbul Technical University in 2008. He received his MSc degree in

materials science and engineering from Koç University in 2011. In 2015, he received his PhD from the University of Twente, for his work on advanced optical imaging with scattering lenses, with Professor Allard Mosk. He is currently a postdoctoral research associate at Yale University, Department of Applied Physics, working with Professor Hui Cao.

**Huzyefe Yılmaz** received his BSc degree in physics from Bilkent University in 2009. He received his MSc degree in physics from Koç University in 2011. He received his PhD in materials science and engineering in 2017 with his work on structural protein-based whispering-gallery mode resonators from the University of Washington, St. Louis, in the group of Professor Lan Yang. Currently, he is a postdoctoral research scientist with Professor Srikanth Singamaneni at the University of Washington, St. Louis.

**Mehmet Selman Tamer** received his BSc in physics from Koç University and MSc degree in physics engineering from Istanbul Technical University. His MSc thesis was on the design and construction of a setup for the detection of tunneling induced photons in a scanning tunneling microscope and an application on gold surfaces. He is currently a PhD student at Delft University of Technology, Department of Precision and Microsystems Engineering.

**Oğuzhan Gürlü** received his BSc degree in physics from Bilkent University, Ankara, in 1999. He received his MSc degree in applied physics from the University of Twente in 2000 with his thesis on an alternative approach to spin polarized scanning tunneling microscopy, and he received his PhD from the University of Twente in 2004 with

his thesis work titled on the platinum covered Si and Ge surfaces under the supervision of Professor Bene Polesema and Professor Harold J. W. Zandvliet. He continued his research at Max Planck Institute Stuttgart at the group of Professor Klaus Kern until 2008. He is currently an associate professor at the Physics Department of Istanbul Technical University.

**Mohammed Sharif Murib** received his BSc in physics from Lebanese University, Faculty of Science, Hadath, in 2005. He joined the MSc program in physics at Koç University in 2007. In 2010, he joined the Bios group at the Institute for Materials Research, Hasselt University, for his PhD, working with Professor Patrick Wagner on bioelectronics and biophotonic sensors. He received his PhD in February 2014. Later, he was an assistant professor of physics at American University of the Middle East, Kuwait. Currently, he is a researcher at the Department of Information Technology (INTEC), Ghent University.

**Ali Serpengüzel** received his PhD degree from Yale University. He is currently a professor of physics and the director of the Microphotonics Research Laboratory, Koç University. His current research focuses on singular or distributed optical microcavities and optical waveguides toward applications in integrated photonics and fiber optics. Other research interests include optical spectroscopy in complex media, nanophotonics, linear and nonlinear optics, and laser diagnostics toward applications in remote sensing, and combustion. He is a fellow member of SPIE, a senior member of IEEE and OSA, and a member of Sigma-Xi.